

SIFT FEATURE BASED DETECTION OF GLAUCOMA

¹APEKSHA AVINASH, ²K.MAGESH, ³C. VINOTH KUMAR

^{1,2,3}Department of ECE, SSN College of Engineering, Chennai, India
E-mail: ¹apeksha13008@ece.ssn.edu.in, ²magesh13053@ece.ssn.edu.in, ³vinothkumarc@ssn.edu.in

Abstract— The normal and glaucomatous fundus images are classified using Support Vector Machines (SVM) and Naïve Bayes in this paper. The features of both classes of images are extracted using the Scale Invariant Feature Transform (SIFT). Two optimal features are then utilized by the SVM Classifier to classify the images into the two respective categories and its performance is compared with that of the Naive Bayes classifier.

Keywords— Glaucoma, Naïve Bayes, Scale Invariant Feature Transform, Support Vector Machine.

I. INTRODUCTION

The number of people (age between 40 and 80 years) with glaucoma worldwide was estimated to be 64.3 million in 2013 with an estimated increase to 76.0 million in 2020 and 111.8 million in 2040 [1]. Glaucoma is a multi-factorial, complex eye disease whose specific characteristics are optic nerve damage and loss of vision that begins with peripheral or side vision. It is often associated with an increase of pressure build-up inside the eye, called intraocular pressure or IOP. This damages the optic nerve which transmits images to the brain, and continued damage will progressively lead to permanent blindness. Although this is usually the cause, even patients with normal range IOP can develop glaucoma. There is no specific threshold of elevated eye pressure that definitely leads to glaucoma; conversely, there is no lower level of IOP that will absolutely eliminate a person's risk of developing glaucoma. That is why early diagnosis and treatment of glaucoma is the key to preventing vision loss.

Since an early onset of Glaucoma does not have any visible symptoms or pain associated with the eye until the later stages, it is important that the disease be correctly identified. Regular glaucoma check-ups include two routine eye tests – Tonometry and Ophthalmoscopy. However, these tests require the services of a doctor or a technician, small instruments and are altogether time-consuming. A better approach would be the use of automated techniques such as Scanning Laser Polarimetry, Optical Coherence Tomography and Heidelberg Retinal Tomography (HRT) [2, 3, 9, 10]. The damage to the Optic Nerve Head (ONH) and the Retinal Nerve Fiber Layer (RNFL) thicknesses are usually the indicators used in these techniques. From the examinations conducted by Quigley, Harry A., et al. [4], it was concluded that the RNFL thickness was a better indicator than colour disc evaluation for the detection of progressive glaucoma damage at an early stage. The position of the nerve fiber layer defects highly correlated with the location of subsequent visual field loss. Results from [6] suggest that RNFL imaging with scanning laser polarimetry had a better performance over HRT for

detecting early occurrences of glaucoma in patients suspected of having the disease.

Since optic nerve damage due to glaucoma has misleadingly been associated with high cup-to-disc ratios (CDRs) [5], Salam, Anum Abdul, et al. [7] proposed a novel methodology of using CDR along with hybrid textural and intensity features to classify retinal fundus images into glaucoma, non-glaucoma and suspect. Fundoscopy is a part of routine eye examination that is useful in detecting structural changes in the eye and thus helps diagnose diseases of the optic nerve like glaucoma. In this paper, retinal fundus image sets are used for training and testing classifiers to categorize them into Normal and Glaucoma. The features of the fundus images are extracted using Scale Invariant Feature Transform (SIFT) and fed into two classifiers: (1) SVM and (2) Naive Bayes, whose performances in correctly categorizing the images are compared in this paper.

II. SCALE-INVARIANT FEATURE TRANSFORM

Feature extraction from the retinal images is carried out by using SIFT. The features extracted using this transform are found to be invariant to image scaling, translation and rotation and are found to be provide robust matching across a substantial range of affine distortion, change in 3D viewpoint, addition of noise, and change in illumination. The features obtained also prove to be highly distinctive and can be used to perform image classification against a large database of features from many images [11]. The SIFT approach generates a large number of features across the image dimensions. These extracted features are compared against the features that are stored in the database. This forms the basis of object recognition and matching. This is one of the most significant applications of Scale Invariant Feature Transform.

The SIFT has four main stages of implementation. This transform employs a cascade filtering approach for extraction and selection of features where expensive operations are performed only on locations which pass few initial tests. The initial implementation

stage carries out the repeated convolution of only scale space kernel - the Gaussian function [13], [14] with the images of each of the selected octaves in both horizontal and vertical directions with a fixed smoothing factor to produce a set of scale-space images. These adjacent scale space images are subtracted to form Difference of Gaussian (DOG) function. From the DOG function, potential extreme points that can be invariant to scaling and change in orientation are located. We can detect the most stable and useful subset of extrema, even with a coarse sampling of scales.

In the second stage of computation, stability is the major criterion used to select the key points. A detailed model is fit at each candidate location, to determine the location and scale.

In the next stage, each candidate location is assigned the location, the scale and the orientation based on local gradient properties which provide invariance to these parameters.

Finally, around each key point, the local image gradients are measured at the selected scale and these gradients are presented in a way that allows significant levels of local shape distortion and change in illumination. Thus, the image data is converted into scale-invariant coordinates in SIFT. The features that are calculated from SIFT are given below.

1. Mean: Mean of the feature set refers to the arithmetic average of the given set.

$$\text{Mean}(X): \mu = \frac{\sum Xi}{N} \quad (1)$$

2. Variance: It is a measurement of the spread between values in the feature set i.e., howfar each data is from the mean.

$$\text{Var}(X): s^2 = \frac{\sum (xi-x)^2}{n-1} \quad (2)$$

3. Skewness: Skewness is a measure of the asymmetry of the probability distribution of a real-valued random variable about its mean. The skewness value can be positive or negative, or even undefined.

$$\text{skewness}(X) = \frac{E[(X-\mu)^3]}{\sigma^3} \quad (3)$$

4. Kurtosis: It is a measure of whether the data is heavy-tailed or light-tailed relative to a normal distribution. That is, data sets with a high kurtosis value tend to have heavy tails or, outliers. Data sets with a low Kurtosis value tend to have light tails or, lack of outliers. A uniform distribution would be an extreme case.

$$\text{kurtosis}(X) = \frac{E[(X-\mu)^4]}{\sigma^4} \quad (4)$$

III. CLASSIFICATION

Once the features are calculated, classification is the next step. Classification algorithms are utilized for the identification of images. These algorithms are based on the assumption that the image in question depicts one or more features and that each of these features belongs to one of several distinct and exclusive classes. The classes may be specified a priori (as in supervised classification) or automatically clustered (as in unsupervised classification) into sets of prototype classes, where only the number of desired categories is specified.

A. Support Vector Machines

Support Vector Machines (SVM) are based on statistical learning theory. The feature set of our training data is first supplied to the SVM classifier. Using this data, the classifier tries to estimate a function that will help distribute the images between the two categories or classes namely 'Normal' and 'Glaucoma'. The next step for the classifier is to identify an optimal hyperplane (corresponding to that decision function) which exists in the middle of the largest margin between the two classes. The training patterns that lie on the margins are called support vectors and they carry all the relevant information about the classification problem.

When the testing data set is fed into the classifier, SVM uses the support vectors identified during training to sort the test images into the correct classes. However, a minimal error during the training phase does not guarantee a correspondingly small error during the testing phase. This is where statistical learning theory comes into play. It is important to restrict the class of functions that SVM can implement to one with a capacity that is suitable for the amount of available training data. SVMs are widely used for classification purposes. It is simple, robust and practical. Also, with the choice of different kernel functions, one can obtain different architectures such as polynomial classifiers, RBF classifiers, and three-layer neural nets [15, 16].

B. Naïve Bayes

The Naive Bayes classifier[17] uses Bayes' Theorem of probability to classify images. Once the features of the training set are fed into the classifier, the probabilities of individual features being present, given the outcome (i.e. the class - 'Normal' or 'Glaucoma') as well as the probabilities of each of the two classes are calculated. Based on these probabilities, the images of the testing set are classified using the formula given below:

$$P(\text{outcome}|\text{evidence}) :$$

$$\frac{P(\text{Likelihood of Evidence})x \text{Prior probability of outcome}}{P(\text{Evidence})} \quad (5)$$

IV. SIMULATION RESULTS

The following section outlines the results obtained during the various stages of simulation. The feature extraction and classification have been implemented using MATLAB 2012a. A set of 15 normal images and 15 glaucomatous images were taken from the FAU database.

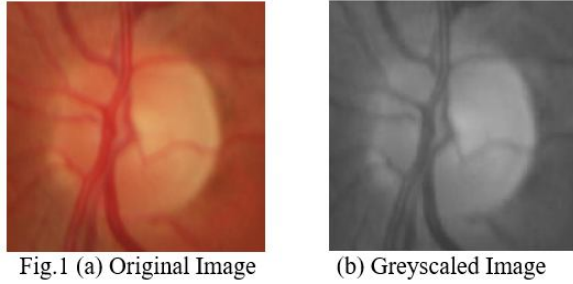


Fig.1 (a) shows the original image while Fig.1 (b) is the greyscale converted image.

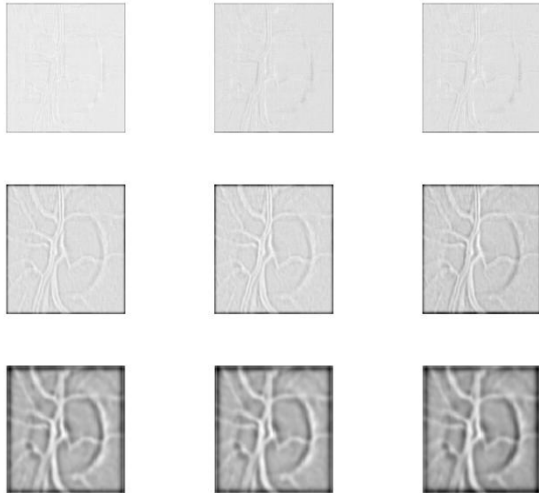


Fig.2 Results of the difference of Gaussian function

Fig.2 depicts the cascaded convolution of the separable Gaussian function with the input grayscale image in horizontal and vertical direction with three octaves and smoothing factor $\sqrt{2}$. The adjacent scale space images thus formed are subtracted to from the Difference of Gaussian function..

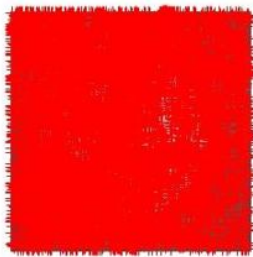


Fig.3 Keypoint Localization

Fig.3 is obtained by identifying keypoints based on their measures of stability. The keypoints are shown as red pluses on the original grayscale image. As seen in Fig.3 above, there are an excessive number of keypoints identified. Therefore, to reduce this large number of keypoints, keypoints with low contrast and poor edge localization are eliminated. Fig.4 (a) and (b) show the reduced accurate keypoints in green and blue respectively.

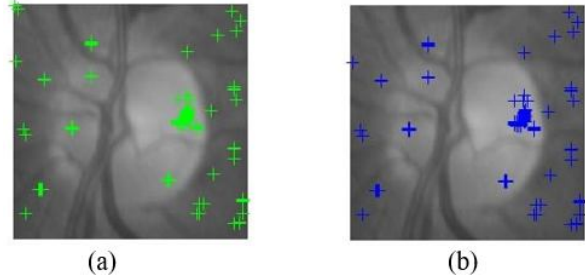


Fig.4 Accurately Localized Keypoints

The features obtained as shown in Fig.4 (blue points) are fed into the SVM and Naïve Bayes Classifiers and the resulting accuracies obtained have been tabulated as shown in Table I and Table II. The performance measures are:

$$\text{True Positive Rate, TPR} = \text{TP} / (\text{TP} + \text{FN}) \quad (6)$$

$$\text{True Negative Rate, TNR} = \text{TN} / (\text{FP} + \text{TN}) \quad (7)$$

$$\text{False Positive Rate, FPR} = \text{FP} / (\text{FP} + \text{TN}) \quad (8)$$

$$\text{False Negative Rate, FNR} = \text{FN} / (\text{TP} + \text{FN}) \quad (9)$$

$$\text{Accuracy, ACC} = (\text{TP} + \text{TN}) / (\text{TP} + \text{FP} + \text{FN} + \text{TN}) \quad (10)$$

$$\text{Precision Predictive Value, PPV} = \text{TP} / (\text{TP} + \text{FP}) \quad (11)$$

where

TP - True Positive (Correctly identified)

TN - True Negative (Correctly rejected)

FP - False Positive (Incorrectly selected)

FN - False Negative (Incorrectly rejected)

are determined by the classification performed by the classifier.

Table I. SVM Classifier Results

Features	TPR	TNR	FPR	FNR	ACC	PPV
Mean& Variance	80.07	66.67	33.33	20.03	73.33	70.55
Mean& Skewness	93.33	80.02	20.06	6.67	86.67	82.35
Mean& Kurtosis	93.33	86.67	13.33	6.67	90.02	87.50
Variance& Skewness	100.00	86.67	13.33	0.00	93.33	88.24
Variance& Kurtosis	93.33	86.67	13.33	6.67	90.07	87.50
Skewness& Kurtosis	80.02	80.03	20.01	20.07	80.02	80.03

Table II. Naïve Bayes Classifier Results

Features	TPR	TNR	FPR	FNR	ACC	PPV
Mean	86.67	46.67	53.33	13.33	66.67	61.97
Variance	73.33	80.01	20.02	26.67	76.67	78.59
Skewness	80.05	80.01	20.08	20.03	80.01	80.05
Kurtosis	80.06	86.67	13.33	20.11	83.33	85.71

SVM Classifier requires two features as input and hence the results taking two at a time are shown. The highest accuracy of correctly classifying the Normal and Glaucomatous images into their respective classes for this image set of 30 images is 93.33% with a False Positive Rate of 13.33% and a False Negative Rate of 0.

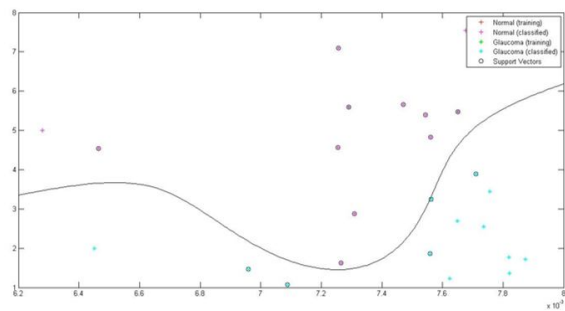


Fig.5 SVM Classification for Variance and Skewness of the SIFT features

The Naïve Bayes classifier takes only one feature as input. The highest accuracy is obtained from the Kurtosis of the SIFT features and is 83.33%. The False Positive Rate is 13.33% and the False Negative Rate is 20%. Thus it can be seen that for the same feature set, the SVM classifier provides a better accuracy of sorting the 30 images into their respective classes.

CONCLUSION

This paper has described the methodology for classifying a composite set of images into two different classes based on the SIFT keypoints extracted from the images. These keypoints have attained significance due to their invariance to scale, image rotation and their robustness across range of illumination variation and affine rotation. This paper has made use of classifiers such as Support Vector Machine and Naïve Bayes to classify the images into their respective classes-Normal and Glaucomatous, based on the SIFT features. The performance of each of the classification carried out by the classifiers is evaluated and the accuracy of classification is compared. The classification performed by the SVM classifier is found to be more accurate(93.33%

accuracy) compared to that of the Naive Bayes classifier(83.33% accuracy). Further research have to be carried out to utilize the chromatic characteristics and texture characteristics of the images while optimizing the SIFT keypoints in the place of monochromatic or gray-scale level manipulations.

REFERENCES

- [1] Tham, Yih-Chung, et al. "Global prevalence of glaucoma and projections of glaucoma burden through 2040: a systematic review and meta-analysis." *Ophthalmology* 121.11 (2014): 2081-2090.
- [2] Tribble, John R., Richard O. Schultz, James C. Robinson, and Terri L. Rothe. "Accuracy of scanning laser polarimetry in the diagnosis of glaucoma." *Archives of Ophthalmology* 117, no. 10 (1999): 1298-1304.
- [3] Weinreb, Robert N., et al. "Detection of glaucoma with scanning laser polarimetry." *Archives of ophthalmology* 116.12 (1998): 1583-1589.
- [4] Quigley, Harry A., et al. "An evaluation of optic disc and nerve fiber layer examinations in monitoring progression of early glaucoma damage." *Ophthalmology* 99.1 (1992): 19-28.
- [5] Sonas, Jost B., Martin C. Fernandez, and Cottfried OH Naumann. "Glaucomatous optic nerve atrophy in small discs with low cup-to-disc ratios." *Ophthalmology* 97, no. 9 (1990): 1211-1215.
- [6] Medeiros, Felipe A., et al. "Comparison of retinal nerve fiber layer and optic disc imaging for diagnosing glaucoma in patients suspected of having the disease." *Ophthalmology* 115.8 (2008): 1340-1346.
- [7] Salam, Anum Abdul, et al. "Autonomous Glaucoma detection from fundus image using cup to disc ratio and hybrid features." 2015 IEEE International Symposium on Signal Processing and Information Technology (ISSPIT). IEEE, 2015.
- [8] Schuman, Joel S., et al. "Optical coherence tomography: a new tool for glaucoma diagnosis." *Current opinion in ophthalmology* 6.2 (1995): 89-95.
- [9] Medeiros, Felipe A., et al. "Evaluation of retinal nerve fiber layer, optic nerve head, and macular thickness measurements for glaucoma detection using optical coherence tomography." *American journal of ophthalmology* 139.1 (2005): 44-55.
- [10] Mistlberger, Andrea, et al. "Heidelberg retina tomography and optical coherence tomography in normal, ocular-hypertensive, and glaucomatous eyes." *Ophthalmology* 106.10 (1999): 2027-2032.
- [11] Lowe, David G. "Distinctive image features from scale-invariant keypoints." *International journal of computer vision* 60.2 (2004): 91-110.
- [12] Hough, Paul VC. *Method and means for recognizing complex patterns*. No. US 3069654. 1962.
- [13] Lindeberg, Tony. "Scale-space theory: A basic tool for analyzing structures at different scales." *Journal of applied statistics* 21.1-2 (1994): 225-270.
- [14] Koenderink, Jan J. "The structure of images." *Biological cybernetics* 50.5 (1984): 363-370.
- [15] Hearst, Marti A., et al. "Support vector machines." *Intelligent Systems and their Applications, IEEE* 13.4 (1998): 18-28.
- [16] Burges, Christopher JC. "A tutorial on support vector machines for pattern recognition." *Data mining and knowledge discovery* 2.2 (1998): 121-167.
- [17] Rish, Irina. "An empirical study of the naive Bayes classifier." *IJCAI 2001 workshop on empirical methods in artificial intelligence*. Vol. 3. No. 22. IBM New York, 2001.

★★★